Evaluation of hysteresis models for predicting the boundary wetting curve

D. G. Fredlund, S. L. Barbour and H. Q. Pham
Civil Engineering Department, University of Saskatchewan, Saskatchewan, Canada

Second Asian Conference on Unsaturated Soils
UNSAT-ASIA 2003, April 15-17, Osaka, Japan

ABSTRACT: Five hysteresis models for the soil-water characteristic curve (SWCC) were selected for comparison in this paper. The comparison is based on 34 soil datasets and the statistical criteria: *R squared value* and *absolute percentage deviation*. The results show that the Feng and Fredlund (1999) model appears to be the simplest and the most appropriate model for predicting the boundary wetting curve once the boundary drying curve has been measured. The other models can accurately predict the boundary wetting curve in some cases.

1 INTRODUCTION

Soil-water characteristic curves have been used to estimate the coefficient of permeability and shear strength functions used to model unsaturated soil behavior (Barbour, 1998; Fredlund and Rahardjo, 1993). The hysteretic nature of the SWCC has been known for many decades but in most routine engineering and agriculture applications only the drying curve has been used due to the complicated nature of most hysteresis models.

There have been a number of studies that have compared the performance of various models to predict the hysteretic behaviour of the SWCC. These comparisons have generally focused on the prediction of scanning curves (Jaynes 1984; Viaene *et al.* 1994; Pham *et al.* 2001a). However, most models require at least two boundary curves in order to predict scanning curves. Five hysteresis models for predicting the boundary wetting curve were selected for evaluation in this paper. These models were selected primarily because of their relative simplicity and the limited amount of data that is required for calibration. The following models are compared: Mualem (1977) model; Mualem (1984) independent model; Hogarth *et al.* (1988) model; Feng and Fredlund (1999) model; and the simplified version of the Feng and Fredlund (1999) model.

2 LITERATURE REVIEW AND THEORY

The models that have been proposed to predict the boundary drying or the boundary wetting curves can be divided into two categories; namely, empirical models and domain models. The empirical models use soil-water characteristic curve-fitting equations and the basic shapes of the SWCC to estimate the hysteretic curves (Scott *et al.*, 1983; Nimmo, 1992; Feng and Fredlund, 1999; Kawai *et al.*, 2000). Domain models assume that there are two states when the pores of a soil are either filled or empty. These states can be described as follows:

- when soil suction, ψ, increases to a certain suction value, ψ_d, then the pore is drained spontaneously, and,
- when soil suction, ψ, decreases to a certain value, ψ_w, then the pore is filled spontaneously ($\psi_w \leq \psi_d$).

A domain model describes the drying and the wetting processes of a soil using a diagram such as a Néel (1942, 1943) diagram or a Mualem (1974) diagram (i.e., Poulovassilis, 1962; Topp, 1971a; Palange, 1980; Mualem, 1973, 1974, 1977, 1984). Details of these diagrams are described in the literature cited above.

2.1 *Mualem (1977) model*

The Mualem (1977) model is a domain model that requires the boundary drying curve and two meeting points, where the boundary drying and the boundary wetting curves coalesce, to predict the entire boundary wetting curve. The Mualem (1977) model is a simplification of the Mualem (1974) model which

uses the Mualem (1974) diagram to describe the hysteretic process. The Mualem (1977) model uses the term *effective degree of saturation* to describe the water content in the soil. The effective degree of saturation can be calculated using equation (1).

$$S^e = \frac{[\theta - \theta_{min}]}{[\theta_u - \theta_{min})]} \quad (1)$$

where θ_u = volumetric water content at the meeting point of the two boundary curves at low soil suction (i.e., close to the *air entry value*); and θ_{min} = volumetric water content at the meeting point of the two boundary curves at high soil suction (i.e., close to the *residual soil suction*).

The Mualem (1977) model expresses the relationship between the boundary drying curve and the boundary wetting curve using equation (2).

$$S_w^e(\psi) = 1 - [1 - S_d^e(\psi)]^{1/2} \quad (2)$$

where S_d^e = effective degree of saturation along the boundary drying curve; and S_w^e = effective degree of saturation along the boundary wetting curve.

2.2 *Mualem (1984) model*

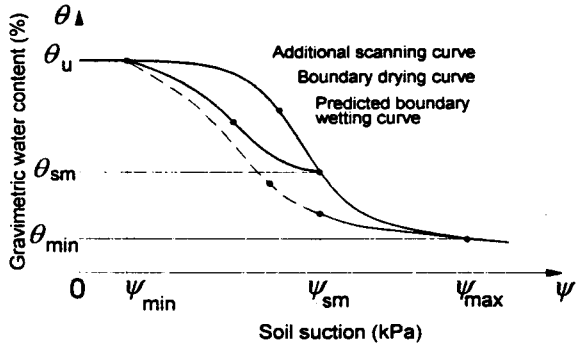

Fig 1. Schematic illustration of predicting boundary wetting curve using Mualem (1984) independent model.

The Mualem independent (1984) model is an improvement of the Mualem (1977) model. In addition to the boundary drying curve and the two meeting points of the two boundary curves, an additional wetting-scanning curve is used to predict the boundary wetting curve (Figure. 1). Considerable mathematical effort is required to obtain the relationships between the scanning curves and the two boundary hysteresis curves.

Mualem (1984) presented mathematical transformations to obtain the relationships between a scanning curve and two boundary curves. A detailed explanation of the Mualem (1984) model can be found in the original paper. The predicted boundary wetting curve consists of two parts: from zero soil suction to the soil suction at the starting point of the scanning curve, and at values of soil suction greater than the soil suction at the starting point of the scanning curve. The first part of the predicted boundary wetting curve is predicted using both the boundary drying curve and the scanning curve, while the second part is predicted using only the boundary drying curve as presented in the Mualem (1977) model. The water content along the boundary wetting curve can be expressed as follow:

$$S_w^e(\psi) = 1 - \frac{1 - S_{ws}^e(\psi_{sm}, \psi)}{[1 - S_d^e(\psi_{sm})]^{1/2}} \quad \text{for } \psi_{min} \le \psi \le \psi_{sm}$$

$$S_w^e(\psi) = 1 - [1 - S_d^e(\psi)]^{1/2} \quad \text{for } \psi_{sm} \le \psi \quad (3)$$

where ψ = soil suction; ψ_{sm} = soil suction at the starting point of the additional wetting scanning curve on the boundary drying curve; $S_w^e(\psi)$ = effective degree of saturation along the boundary wetting curve at a soil suction of ψ; $S_d^e(\psi)$ = effective degree of saturation along the boundary drying curve at a soil suction of ψ; and $S_{ws}^e(\psi_{sm}, \psi)$ = effective degree of saturation along the additional wetting-scanning curve at a soil suction of ψ.

2.3 *Hogarth et al. (1988) model*

The Hogarth *et al.* (1988) model is an extension of the Parlange model (1976; 1980) and which uses the Néel (1942;1943) diagram to describe the hysteretic process in soils. By applying the Brooks and Corey (1964) soil-water characteristic curve-fitting equation, mathematical problems near the inflection point in the Parlange (1976; 1980) model are resolved. Similar to the Mualem (1977) model, in addition to the boundary drying curve two meeting points, where the boundary drying and the boundary wetting curves coalesce, are used to predict the entire boundary wetting curve. In order to predict the boundary wetting curve, the boundary drying curve is best-fit using the following equation:

$$\left(\frac{\theta_d(\psi)}{\theta_{ae}}\right) = \left(\frac{\psi_{ae}}{\psi}\right)^{\lambda}\left(1 + \lambda - \lambda\frac{\psi_{we}}{\psi}\right) \quad \text{for } \psi \ge \psi_{ae}$$

$$\theta_d(\psi) = \theta_u, \quad \text{for } \psi \le \psi_{ae} \quad (4)$$

where ψ_{ae} = curve-fitting parameter represents air entry value; ψ_{we} = soil suction at the meeting point of the boundary curves at a relatively low suction, λ = curve-fitting parameter; and $\theta_{ae} = \theta_u / (1 + \lambda - \lambda(\psi_{we}/\psi_{ae}))$

Two curve fitting parameters; ψ_{ae} and λ, are obtained from a "best-fit" of the boundary drying curve. The volumetric water content along the boundary wetting curve can be expressed as follows:

$$\theta_w(\psi)=\theta_{ae}\left[\left(\frac{\psi_{ae}}{\psi}\right)^{\lambda}+\frac{\lambda}{\psi_{\max}}\left(\frac{\psi_{ae}}{\psi_{\max}}\right)^{\lambda}(\psi-\psi_{we})\right] \quad \text{for } \psi\geq\psi_{ae}$$

$$\theta_w(\psi)=\theta_{ae}\left[\left(1+\lambda-\lambda\frac{\psi}{\psi_{ae}}\right)+\frac{\lambda}{\psi_{\max}}\left(\frac{\psi_{ae}}{\psi_{\max}}\right)^{\lambda}(\psi-\psi_{we})\right] \quad \text{for } \psi_{ae}\geq\psi\geq\psi_{we}$$

$$\theta_w(\psi)=\theta_u; \quad \text{for } \psi_{we}\geq\psi \qquad (5)$$

where ψ_{max} = soil suction at the meeting point of the two boundary curves at a relatively high suction.

The two parameters; ψ_{we} and ψ_{max}, are the values of soil suction at the two meeting points of the two boundary curves at relatively low and high suction, respectively. These are the some meeting points as used in the Mualem (1977 and 1984) models.

2.4 *Feng and Fredlund (1999) model*

The Feng and Fredlund (1999) model requires the boundary drying curve and two points on the boundary wetting curve in order to predict entire wetting curve. Both boundary drying curve and boundary wetting curve are presented using the soil-water characteristic curve-fitting equation (6).

$$w(\psi)=\frac{w_u b+c\psi^d}{b+\psi^d} \qquad (6)$$

where w_u = water content on the boundary drying curve at zero soil suction; and b, c, d = curve-fitting parameters.

The residual water content and the water content at zero soil suction (w_u) are assumed to be essentially the same for both of the two boundary curves. Once the boundary drying curve is measured in the laboratory, two curve-fitting parameters for the boundary wetting curve in equation (6) are known (i.e., w_u and c). Two additional curve-fitting parameters; b_w and d_w, are required to predict the boundary wetting curve. In order to find these parameters, two additional points on the boundary drying curve are required. A suggestion for the position of the two points along the boundary wetting curve was presented by (Pham *et al.*, 2002). The position of the first point on the boundary wetting curve can be defined as a point having a soil suction of ψ_1 such that;

$$\psi_1\approx\left(\frac{b}{10}\right)^{\frac{1}{d}} \qquad (7)$$

where b, d are best-fit parameters of the boundary drying curve (equation (6)).

The soil suction at the second additional point, ψ_2, can be determined from equation (8):

$$\psi_2=\psi_1-2\left(\left(\frac{b(w_u-w_1)}{w_1-c}\right)^{\frac{1}{d}}-b^{\frac{1}{d}}\right) \qquad (8)$$

where w_u = water content on the boundary drying curve at zero soil suction; b, c, d = curve fitting parameters of the boundary drying curve; ψ_1 = soil suction at the first additional point; and w_1 = water content at the first additional point.

The two parameters b_w and d_w can then be calculated using equations (9) and (10)

$$d_w=\frac{\log\left(\frac{(w_{1w}-c)(w_u-w_{2w})}{(w_u-w_{1w})(w_{2w}-c)}\right)}{\log(\psi_{2w}/\psi_{1w})} \qquad (9)$$

$$b_w=\frac{(w_{1w}-c)\psi_{1w}^{d_w}}{w_u-w_{1w}} \qquad (10)$$

2.5 *Further simplification of the Feng and Fredlund (1999) model*

The Feng and Fredlund (1999) model requires two additional points on the boundary wetting curve to calculate the slope of the boundary wetting curve and predict the entire boundary wetting curve. The simplified version of the Feng and Fredlund model assumes that the boundary wetting curve and the boundary drying curve are parallel when using algebraic coordinate. Consequently, only one point on the boundary wetting curve is required.

Parameter d controls the slope of the curve in equation (6), since parameter c are the same for the both boundary drying and boundary wetting curves. The boundary wetting curve is assumed to be parallel to the boundary drying curve. The curve-fitting parameter, d_w, for the boundary wetting curve can then be assumed to be the same as parameter d for the boundary drying curve. The curve-fitting parameter b_w from the boundary wetting curve can be calculated using equation (11).

$$b_w=\frac{(w_1-c)\psi_1^{d}}{w_u-\theta_1} \qquad (11)$$

where w_u = water content on the boundary drying curve at zero soil suction; ψ_1, w_1 = soil suction and gravimetric water content of the additional point on the boundary wetting curve, respectively; and c, d = curve-fitting parameters obtained from fitting the boundary drying curve.

3 COMPARISONS OF THE SOIL-WATER HYSTERESIS MODELS

Hysteretic SWCC for 34 different soils were used for the comparison of the models. Only soils having at least two boundary hysteresis curves were selected. Thirty two of the 34 soil datasets were collected from the research literature. Two soil datasets were measured by the authors. The collected soil data was converted to gravimetric water content versus soil suction. Details of these 34 soil datasets were described by Pham (2001b) and only the literature references are found in the Table 1.

Table 1. List of collected soils.

No.	Soil name	Research authors
1	Adelaide Dune Sand	Talsma (1970)
2	Avondale Clay Loam	Watson et al. (1975)
3	Caribou Silt Loam	Topp (1971b)
4	Ceramic (No. 1)	Feng (1999)
5	Coarse Sand	Viaene et al. (1995)
6	Dune Sand	Gillham, Klute and Heermann (1976)
7	Glass Bead (4D)[1]	Nimmo and Miller (1986)
8	Glass Bead (20D)[1]	Nimmo and Miller (1986)
9	Glass Bead (35D)[1]	Nimmo and Miller (1986)
10	Glass Bead (50D)[1]	Nimmo and Miller (1986)
11	Glass Beads	Bomba and Miller (1967)
12	Glass Beads Ballotini	Poulovassilis (1962)
13	Mixed Sand Fraction	Poulovassilis (1970b)
14	Mixed Sand Fraction	Poulovassilis and Ghamry (1978)
15	Molongo Sand	Talsma (1970)
16	Norfolk Sandy Loam (15D)[1]	Hopmans and Dane (1986)
17	Norfolk Sandy Loam (32D)[1]	Hopmans and Dane (1986)
18	Packed Sand	Vachaud and Thony (1971)
19	Plainfield Sand Loam (20D)[1]	Nimmo and Miller (1986)
20	Plainfield Sand Loam (35D)[1]	Nimmo and Miller (1986)
21	Plainfield Sand Loam (50D)[1]	Nimmo and Miller (1986)
22	Plano Silt Loam (4D)[1]	Nimmo and Miller (1986)
23	Plano Silt Loam (35D)[1]	Nimmo and Miller (1986)
24	Plano Silt Loam (50D)[1]	Nimmo and Miller (1986)
25	Porous body I (sand)	Poulovassilis (1970a)
26	Porous body II (sand)	Poulovassilis (1970a)
27	Rideau Clay Loam	Topp (1971b)
28	Rubicon Sandy Loam	Topp (1969)
29	Sand	Poulovassilis and Childs (1971)
30	Sand (No.17)	Perrens and Watson (1977)
31	Sand (R8)	Ayers and Watson (1977)
32	Wray Dune Sand	Mualem and Klute (1984)
33	Beaver Creek sand (Packed)	Laboratory test program
34	Processed Silt (Packed)	Laboratory test program

where: [1] Some soils are tested at different temperatures, the notations: 4D, 15D, 20D, 32D, 35D and 50D mean the temperatures of the samples are 4, 15, 20, 32, 35 and 50 degrees Celsius, respectively.

3.1 *Statistical comparison criteria*

The various hysteresis models were compared both visually and statistically. Two statistical criteria were used to compare the hysteresis models: Absolute percent deviation, *APD*, and *R squared* method. The Absolute percent deviation, *APD*, and the *R squared* method were applied to 100 points generated on the predicted boundary wetting curves of the five models and the actual wetting curves. These 100 points were determined by dividing each boundary wetting curve into 99 equal increments of soil suction. The two criteria were calculated as follow:

- Absolute percent deviation (%):

$$APD(\%) = \sum_{i=1}^{100} Abs\left(\frac{w_{pr}(i) - w_{ms}(i)}{w_{ms}(i)}\right) \tag{12}$$

- R squared:

$$R^2 = \frac{\left(\sum_{i=1}^{100} w_{ms}(i)w_{pr}(i) - \frac{\sum_{i=1}^{100} w_{ms}(i)\sum_{i=1}^{100} w_{pr}(i)}{100}\right)^2}{\left(\sum_{i=1}^{100} w_{pr}^2(i) - \frac{\left(\sum_{i=1}^{100} w_{pr}(i)\right)^2}{100}\right)\left(\sum_{i=1}^{100} w_{ms}^2(i) - \frac{\left(\sum_{i=1}^{100} w_{ms}(i)\right)^2}{100}\right)} \tag{13}$$

where $w_{pr}(i)$ = water content at a point i on the predicted boundary wetting curve; and $w_{ms}(i)$ = water content at a point i on the actual boundary wetting curve.

3.2 *Results and discussion:*

The five models were used to predict the boundary wetting curve for the 34 soil datasets. The results of the five models were then ranked for each soil dataset. Tables 2 and 3 present the ranking of the five models using the two criteria for the soil database. The accuracy of the prediction of each model using each soil dataset was ranked from 1st to 5th. It is seemed that, the Mualem (1984) independent model will provide a less accurate result if an additional wetting-scanning curve starting at a lower soil suction is used. The additional wetting scanning curves selected by the authors for the Mualem independent (1984) model is the available wetting scanning curve

starting at highest soil suction. Of the 34 soils collected for the database, there are only 25 soil datasets having at least one wetting scanning curve. Therefore, the Mualem independent (1984) model only applies to 25 soil datasets. The predicted boundary wetting curves for the Caribou Silt Loam (Topp, 1971) using the five models are presented in Figures. 2 to 6. The results show that the Feng and Fredlund (1999) model appears to be the most accurate and significantly better than the second ranked model (i.e., Mualem independent (1984) model). The last three models: the Hogarth *et al.* (1988) model, the Mualem (1977) model and the simplified version of the Feng and Fredlund (1999) model give accurate results in a number of cases.

An addition advantage of the Feng and Fredlund (1999) model is that the required calibration data is relatively simple and easily measured. In general, it may be necessary to do more than one soil suction increment or soil suction decrement in a laboratory test program to determine the meeting point of the two boundary curves as is required for some of the models (i.e., Hogarth *et al.*, 1988; Mualem models, 1976, 1984). It is more time consuming to determine the meeting points of the two boundary curves than simply two points along the boundary wetting curve. The results also show that there is relatively good agreement between the two statistical criteria (i.e., *absolute percentage deviation* and *R squared*).

Table 2. Ranking of the seven soil-water hysteresis models for predicting the boundary wetting curve based on *Absolute percentage deviation.*

Position	M1*	M2*	M3*	M4*	M5*
1st	2	9	1	20	2
2nd	1	7	16	9	1
3rd	6	6	10	5	7
4th	8	3	6	0	17
5th	17	0	1	0	7
Total	34	25	34	34	34
Average ADP	17.74	6.23	6.91	4.11	10.52

Table 3. Ranking of the seven soil-water hysteresis models for predicting the boundary wetting curve based on *R squared.*

Position	M1*	M2*	M3*	M4*	M5*
1st	0	9	1	23	1
2nd	2	10	13	8	1
3rd	7	6	10	3	8
4th	7	0	7	0	20
5th	18	0	3	0	4
Total	34	25	34	34	34
Average R quared	0.859	0.989	0.976	0.994	0.946

*where M1, M2, M3, M4 and M5 are the Mualem (1977) model, the Mualem (1984) model, the Hogarth *et al.* (1988) model, the Feng and Fredlund (1999) model and the simplified version of the Feng and Fredlund (1999) model, respectively.

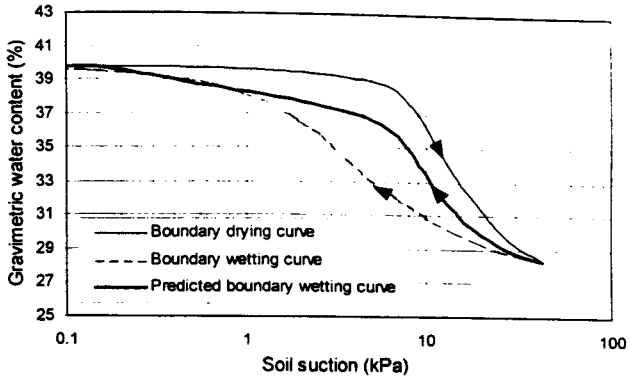

Figure 2. Predicted and measured boundary wetting curves for Caribou Silt Loam (Topp, 1971b) applying the Mualem (1977) model. Continuous lines are the measured curves and the dashed line is the predicted curve.

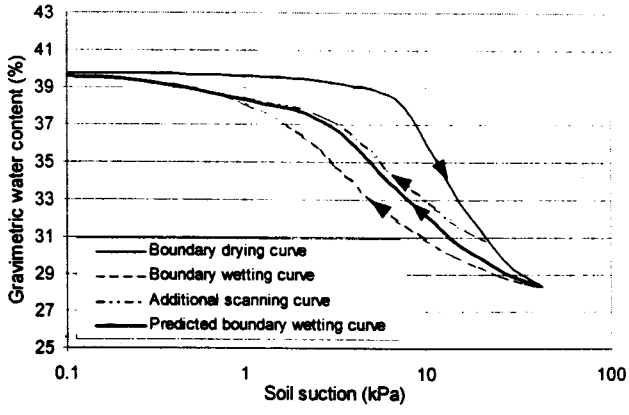

Figure 3. Predicted and measured boundary wetting curves for Caribou Silt Loam (Topp, 1971b) applying the Mualem Independent (1984) model: the continuous lines are the measured curves and the dashed line is the predicted curve.

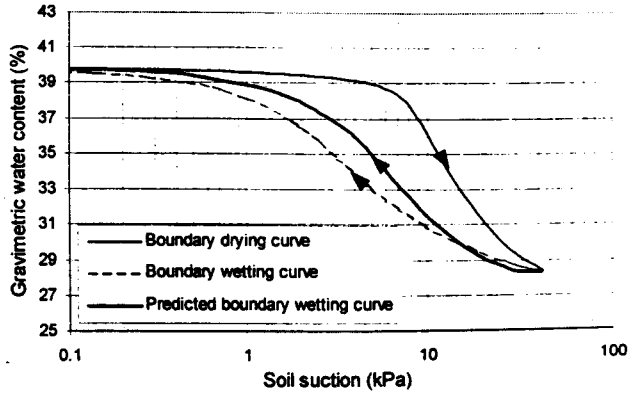

Figure 4. Predicted and measured boundary wetting curves for Caribou Silt Loam (Topp, 1971b) applying the Hogarth et al. (1988) model: the continuous lines are the measured curves and the dashed line is the predicted curve.

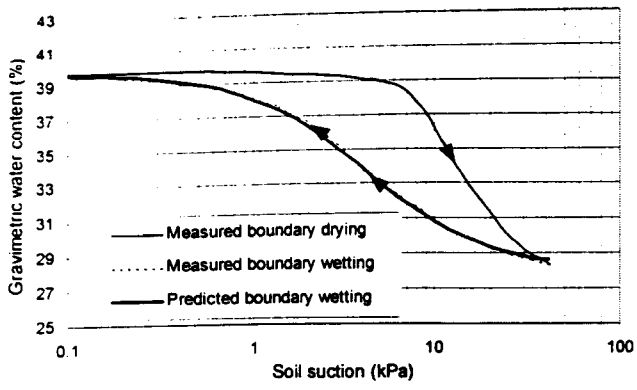

Figure 5. Predicted and measured boundary wetting curves for Caribou Silt Loam (Topp, 1971b) applying the Feng and Fredlund (1999) model: the continuous lines are the measured curves and the dashed line is the predicted curve.

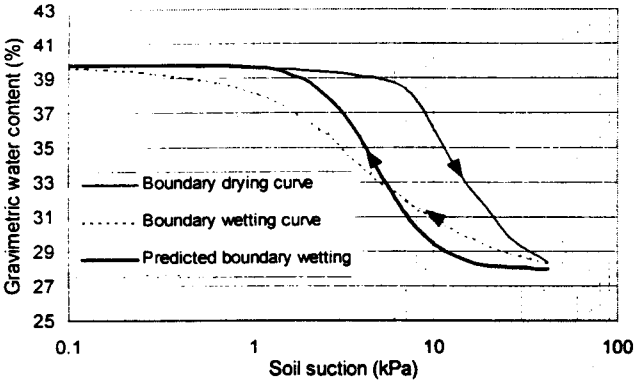

Figure 6. Predicted and measured boundary wetting curves for Caribou Silt Loam (Topp, 1971b) applying the Simplified version of the Feng and Fredlund (1999) model: the continuous lines are the measured curves and the dashed line is the predicted curve.

4 CONCLUSION

From the above study, the following conclusions can be made:

1. The Feng and Fredlund (1999) model is the most appropriate model for predicting the boundary wetting curve. It is recommended to apply the model in engineering practice.
2. The other models such as the Mualem (1977, 1984) models, the Hogarth *et al.* (1988) model and the simplification version of the Feng and Fredlund (1999) model can only apply in a few cases.
3. There is a good agreement in comparing hysteresis models for predicting the boundary wetting curve between two statistical criteria; absolute percent deviation and R squared.

REFERENCES

Barbour, S. Lee. 1998. Nineteenth Canadian Geotechnical Colloquium; the soil-water characteristic curve; a historical perspective. *Canadian Geotechnical Journal*, **35**(5): 873-894.

Feng, M. 1999. The effects of capillary hysteresis on the measurement of matric suction using thermal conductivity sensors. *Master of Science thesis*, University of Saskatchewan, Saskatoon, Canada.

Fredlund, D. G., and Rahardjo, H. 1993. *Soil mechanics for unsaturated soils*. John Wiley and Sons, New York, NY, 1993.

Hogarth, W. L. Hopmans, J., Parlange, J. Y., and Haverkamp, R. 1988. Application of a simple soil-water hysteresis model. *Journal of Hydrology*, **98**: 21-29.

Jaynes, D. B. 1985. Comparison of soil-water hysteresis models. *Journal of Hydrology*, **75**: 287-299.

Kawai, K., Karube, D., and Kato, S. 2000. The model of water retention curve considering effects of void ratio. Proceeding Asian Conference on Unsaturated Soils, pp. 329-334.

Mualem, Y. 1973. Modified approach to capillary hysteresis based on a similarity hypothesis. Water Resources Research, **9**(5): 1324-1331.

Mualem, Y. 1974. A conceptual model of hysteresis. *Water Resources Research*, **10**(3): 514-520.

Mualem, Y. 1977. Extension of the similarity hypothesis used for modeling the soil water characteristics. Water Resources Research, **13**(4): 773-780.

Mualem, Y. 1984. A modified dependent domain theory of hysteresis. *Journal of Soil Science*, **137**(5): 283-291.

Néel, L. 1942. Théorie des lois d'aimantation de Lord Rayleigh, 1. Cahiers de Physique, **12**: 1-20.

Néel, L. 1943. Théorie des lois d'aimantation de Lord Rayleigh, 2. Cahiers de Physique, **13**: 18-30.

Nimmo, J. R. 1992. Semi-empirical model of soil water hysteresis. Soil Science Society of America Journal, **56**: 1723-1730.

Palange, Jean-Yves. 1980. Water transport in soils. Annual Revision of Fluid Mechanics, **12**: 77-102.

Pham, Q. H., Fredlund, D. G., Barbour, S. Lee, 2001a. Evaluation of physically based hysteresis models soil-water characteristic curve. Proceeding of the international conference on management of the land and water resources. Hanoi, October 20-22, pp. 41-48.

Pham, Q. H. 2001b. An Engineering Model of Hysteresis for Soil-Water Characteristic Curves. *Master of Science thesis*, University of Saskatchewan, Saskatoon, Canada.

Pham, Q. H., Fredlund, D. G., Barbour, S. Lee, 2002. A simple soil-water hysteresis model for predicting the boundary wetting curve. Proceeding 55th Canadian Geotechnical Conference - 3rd Joint Iah-Cnc/Cgs Conference, Niagara Falls, Ontario, Canada, Sheraton Fallsview Hotel, October 20-23, 2002.

Scott, P. S., Farquhar, G. J., and Kouwen, N. 1983. Hysteretic effects on net infiltration. Advances in Infiltration, ASAE St. Joseph, MI Publish, **11**: 163-170.

Topp, G. C. 1971a. Soil-water hysteresis: The domain theory extended to pore interaction conditions. Soil Science Society of America Proceeding, **35**: 219-225.

Topp, G. C. 1971b. Soil water hysteresis in silt loam and clay loam soils. Water Resources Research, **7**(4): 914-920.